Conformational Analysis of Poly(propylene sulfide)

Yuji Sasanuma,*,† Yugo Hayashi,† Hiroki Matoba,† Ikuko Touma,† Hajime Ohta,† Misa Sawanobori,† and Akira Kaito‡

Department of Materials Technology, Faculty of Engineering, Chiba University, 1-33 Yayoi-cho, Inage-ku, Chiba 263-8522, Japan, and Macromolecular Technology Research Center, National Institute of Advanced Industrial Science and Technology (AIST), AIST Tokyo Water Front, 2-41-6 Aomi, Kohtoh-ku, Tokyo 135-0064, Japan

Received May 13, 2002; Revised Manuscript Received July 22, 2002

ABSTRACT: Conformational characteristics of poly(propylene sulfide) (PPS, $[CH_2C^*H(CH_3)S]_x$) have been investigated. Proton and carbon-13 NMR vicinal coupling constants observed from its monomeric model compound, 1,2-bis(methylthio)propane (BMTP, $CH_3S-CH_2-C^*H(CH_3)-SCH_3$), were analyzed to yield bond conformations of the S−C, C−C*, and C*−S bonds. Ab initio molecular orbital (MO) calculations at the MP2/6-311+G(3df,2p)//HF/6-31G(d) and B3LYP/6-311+G(3df,2p)//B3LYP/6-31G(d) levels were carried out for BMTP to evaluate free energies and dipole moments of all the possible conformers. Conformational energies and bond dipole moments of BMTP were estimated therefrom. Conformational energies of BMTP and PPS were also determined by simulations based on the rotational isomeric state scheme for experimental observations of bond conformations of BMTP, characteristic ratio of atactic PPS, and dipole moment ratios of isotactic and atactic PPS. The first-order interaction energies for the S−C (E_σ) and the C−C* (E_α and E_β) bonds were obtained as follows: $E_\sigma = -1.0$ to -0.60 kcal mol^{-1}, $E_\alpha = 0.5-0.6$ kcal mol^{-1}, and $E_\beta = 1.1-1.2$ kcal mol^{-1}. The second-order ω_1 and ω_2 interactions, representing intramolecular C−H···S interactions, are repulsive: $E_{\omega 1} = 0.6-0.9$ kcal mol^{-1} and $E_{\omega 2} = 1.0-1.2$ kcal mol^{-1}. The S−C, C−C*, and C*−S bonds were found to prefer the gauche, trans, and trans states, respectively. The conformational characteristics of unperturbed PPS are similar to those of poly(ethylene sulfide) but significantly different from those of its corresponding polyether, poly(propylene oxide) (PPO), although isotactic PPS and PPO are isomorphous. The conformational characteristics of PPS are discussed in terms of solvent effect, crystal structure, and thermal properties.

Introduction

The S−C bond of poly(methylene sulfide) (PMS) exhibits a strong gauche preference, as found in the C−O bond of poly(methylene oxide) (PMO).[1] The gauche stabilization, being due to antiparallel dipole−dipole interaction and n_S (lone pair) → σ^*_{C-S} (antibonding orbital) hyperconjugation, was evaluated by ^{13}C NMR to be −1.4 to −1.0 kcal mol^{-1}. In our previous paper[2] (hereafter referred to as paper I), the C−S and C−C bonds of poly(ethylene sulfide) (PES) were shown to prefer gauche and trans states, respectively. By the natural bond orbital analysis[3] on PES, the gauche stability (−0.7 to −0.4 kcal mol^{-1}) of the C−S bond was indicated to come mainly from $n_S \rightarrow \sigma^*_{C-C}$ delocalization. The trans preference (0.3−0.4 kcal mol^{-1}) of the C−C bond results from a steric S···S repulsion occurring in the gauche conformation. In the crystal, the S−C−C−S bond sequence of PES adopts $g^\pm t g^\mp$ conformations,[4] in which electron density in antibonding σ^*_{C-S} and σ^*_{C-C} orbitals is maximized and favorable intramolecular dipole−dipole interactions are formed. Accordingly, PES has conformational characteristics different from poly(ethylene oxide) (PEO), of which O−C−C−O bonds take either the tgt or the ttt form in the crystal.[5,6] Melting points of PMS and PES are respectively 245 and 216 °C, being much higher than those of PMO (180 °C) and PEO (68 °C). The high melting points of polysulfides were suggested to come from enthalpy of fusion, in other words, strong intermolecular interactions in the crystals.[2,7] Conformations of these polysulfides, of which electrons are so flexible as to reduce steric repulsions and enhance favorable dipole−dipole interactions, may be easily perturbed by solvents; the conformational energies are apt to vary with solvent.[1,2]

Poly(propylene sulfide) (PPS, $[CH_2C^*H(CH_3)S]_x$, Figure 1a) adopts all-trans conformation in the crystal.[8] The melting point (53 °C) is much lower than those of PMS and PES. In contrast to PMS and PES, PPS is soluble in a variety of solvents.[9] Therefore, its configuration-dependent properties such as characteristic ratio[10] and dipole moment ratio[11,12] have been reported. Since PPS has an asymmetric carbon (denoted by asterisk) in the repeating unit, it has two stereochemical arrangements, that is, (*R*)- and (*S*)-optical isomers. In this paper, (*R*)-isomers are mostly used as models for isotactic PPS and its model compounds. Arguments stated here are also valid for the (*S*)-forms.

In this study, we measured ^{1}H and ^{13}C NMR of a monomeric model compound, 1,2-bis(methylthio)propane (BMTP, $CH_3SCH_2C^*H(CH_3)SCH_3$, Figure 1b) and analyzed vicinal coupling constants (^3J's) to evaluate bond conformations of the S−C, C−C*, and C*−S bonds. These experiments have the following advantages. (1) The NMR method allows us to determine bond conformations for the individual bonds. (2) The small model compound gives spectra of higher quality than the polymer itself. (3) The conformation of a polymer in the Θ state may be interpreted in terms of only short-range intramolecular interactions; conformational energies are expected to be common to the polymer and its model compounds.

* To whom correspondence should be addressed. E-mail: sasanuma@tc.chiba-u.ac.jp. Fax: +81 43 290 3394.
† Chiba University.
‡ AIST.

10.1021/ma020730m CCC: $22.00
Published on Web 09/11/2002

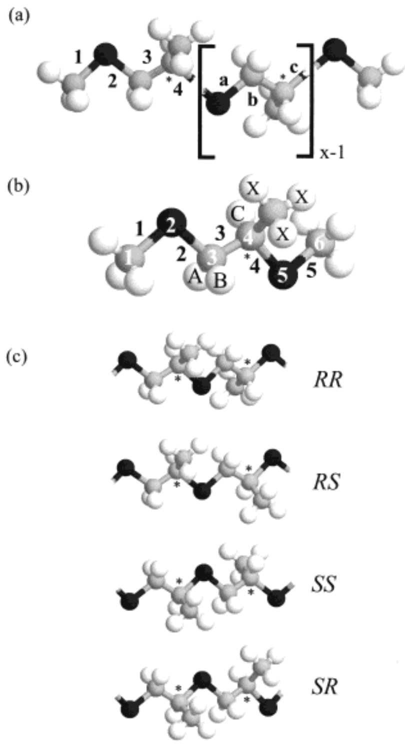

Figure 1. (a) Poly(propylene sulfide) (PPS), (b) 1,2-bis-(methylthio)propane (BMTP), and (c) linkage types between adjacent repeating units. (*R*)-Isomers are used as models for BMTP and isotactic PPS. The bonds and atoms are designated as indicated, and *x* is the degree of polymerization. The asterisks indicate the asymmetrical carbons.

Ab initio molecular orbital (MO) calculations on BMTP were carried out to evaluate free energies, atomic charges, and dipole moments of all the possible conformers. The conformational energies of PPS were determined from experimental observations of bond conformations of BMTP, characteristic ratio of atactic PPS, and dipole moment ratios of atactic and isotactic PPS. In this paper, the conformational characteristics of PPS, revealed from these theoretical and experimental analyses, are compared with those of related polysulfides and polyethers and discussed in terms of solvent effect, crystal structure, and thermal properties.

Materials and Methods

Preparation of BMTP. Aqueous solution of sodium thiomethoxide (0.32 mol, 135 mL) was heated to 60 °C in a four-necked flask with a condenser, a thermometer, and a dropping funnel. To the solution, water (15 mL), trioctylmethylammonium chloride (1.0 g), and 1,2-dibromopropane (0.14 mol, 15 mL) were added dropwise.[13] The mixture was heated at 60 °C for ca. 6 h. After being cooled to room temperature, the reaction mixture was subjected to extraction with ether. The organic extract was dried over sodium sulfate for a day, filtered, condensed, and distilled to yield BMTP (bp 76 °C, yield 60%). The ^{1}H NMR parameters are given in the caption of Figure 2. Preparation of 2-(1,1-dimethylethyl)-1,4-dithiane (DMEDT) has been reported in paper I.

NMR Measurements. ^{1}H (^{13}C) NMR spectra were measured at 500 MHz (125.65 MHz) on a JEOL JNM-LA500 spectrometer equipped with a variable temperature controller. During the measurement the probe temperature was maintained within ±0.1 °C fluctuations. In the measurements, free induction decays were accumulated eight (ca. 6000) times. The $\pi/2$ pulse width, data acquisition time, and recycle delay were 5.6 (4.8) μs, 16.4 (10.4) s, and 3.7 (2.5) s, respectively. Here, the values in the parentheses represent ^{13}C NMR parameters.

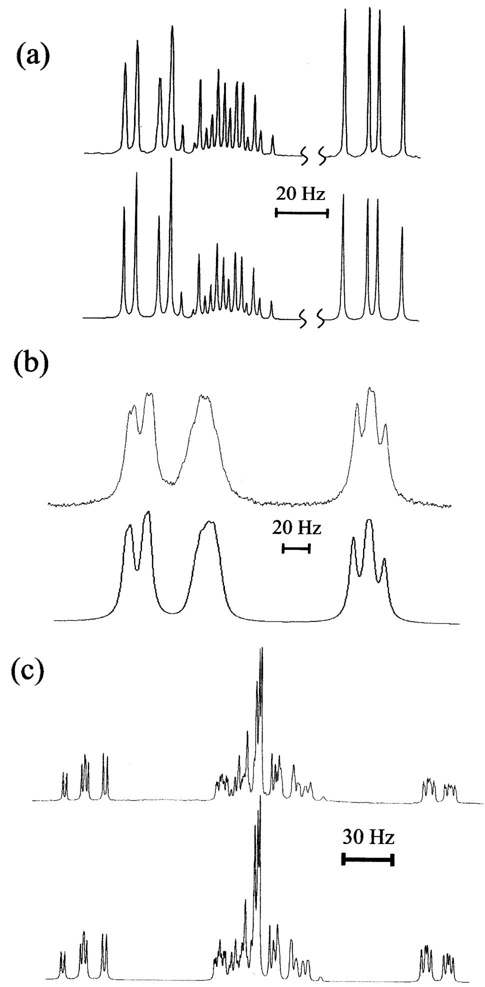

Figure 2. Observed (above) and calculated (below) ^{1}H NMR spectra: (a) BMTP in C_6D_6 at 26 °C; (b) BMTP in the gas phase at 150 °C; (c) DMEDT in C_6D_{12} at 25 °C. Proton NMR parameters on spectra a are as follows: chemical shifts, $\nu_A - \nu_B = 169.87$ Hz, $\nu_A - \nu_C = 32.34$ Hz, and $\nu_A - \nu_X = 701.69$ Hz; coupling constants, $^2J_{AB} = -13.39$ Hz, $^3J_{AC} = 4.40$ Hz, $^3J_{BC} = 9.57$ H, and $^3J_{CX} = 6.83$ Hz (for designation of protons, see Figure 1b).

In the ^{13}C NMR measurements, the gated decoupling technique was used.

In the NMR measurements for solution samples, cyclohexane-d_{12}, benzene-d_6, and dimethyl sulfoxide-d_6 (DMSO-d_6) were used as the solvents, and the solute concentration was ca. 5 vol %. Standard NMR glass tubes of 5 mm o.d. were used. The sample for the gas-phase measurements was prepared as described previously.[1] The vapor pressure in the NMR tube at 150 °C was roughly estimated as follows. The enthalpy of vaporization (ΔH_{vap}) of BMTP may be approximated as 29.7 kJ mol^{-1} by Trouton's rule: $\Delta H_{vap}/T_{bp} \simeq 85$ J mol^{-1} K^{-1}, where T_{bp} is the boiling point (349.2 K) of BMTP at 1 atm. The substitution of the ΔH_{vap} value into the Clausius−Clapeyron equation yields a vapor pressure of 5.9 atm at 150 °C. Thus, the inner pressure of the sample tube may be estimated as 7.1 atm (the sum of vapor and atmospheric (1.2 atm at 150 °C) pressures).

Ab Initio MO Calculations. Ab initio MO calculations were carried out for BMTP using the Gaussian98 program[14] installed on a Compaq XP1000 workstation. At the HF/6-31G(d) level, the geometrical parameters were fully optimized, and zero-point energies, thermal energies, and entropies were also calculated for all the possible conformers. Then, a scale factor of 0.9135 was used to correct the thermodynamic quantities.[15] With the geometries thus determined, the self-consistent field (SCF) energies were calculated at the MP2/6-311+G(3df, 2p) level (abbreviated as MP2/6-311+G(3df, 2p)//HF/6-31G(d)); the

Table 1. Observed Vicinal $^1H-^1H$ and $^{13}C-^1H$ Coupling Constants of BMTP

medium	dielectric constant of medium[a]	temp (°C)	$^3J_{AC}$ (Hz)	$^3J_{BC}$ (Hz)	$^3J_{CH_A}$ (Hz)	$^3J_{CH_B}$ (Hz)	$^3J_{CH_C}$ (Hz)
gas	1.00	150	3.8 ± 0.4	10.0 ± 0.4			
cyclohexane-d_{12}	2.02	10.0	3.95	10.19	4.17	5.47	3.55
		26.0	4.06	9.99	4.17	5.40	3.59
		43.0	4.15	9.80	4.19	5.34	3.60
		59.0	4.29	9.66	4.20	5.26	3.65
		75.0	4.35	9.51	4.20	5.22	3.65
benzene-d_6	2.28	10.0	4.36	9.69	4.06	5.26	3.51
		26.0	4.40	9.57	4.07	5.22	3.52
		43.0	4.56	9.44	4.09	5.15	3.53
		59.0	4.53	9.36	4.09	5.11	3.53
		75.0	4.56	9.03	4.09	5.07	3.51
dimethyl sulfoxide-d_6	45.0	25.0	4.71	9.13	4.01	5.12	3.31
		41.0	4.78	8.99	4.04	5.07	3.37
		58.0	4.94	8.86	4.06	5.01	3.39
		74.0	4.97	8.73	4.09	4.97	3.45
		90.0	4.98	8.66	4.13	4.91	3.48

[a] At 20 °C.

atomic charges and dipole moments were computed by the Merz–Singh–Kollman method.[16,17] As stated above, the inner pressure of the NMR tube was estimated as 7.1 atm. However, this is a crude estimate based on Trouton's rule. To investigate the pressure dependence of bond conformations of BMTP, the conformer free energies at 150 °C and 7.1 atm, at 150 °C and 1.0 atm, and at 25 °C and 1.0 atm were calculated from the SCF energy and thermodynamic quantities. These computations were also carried out at the B3LYP/6-311+G(3df, 2p)//B3LYP/6-31G(d) level. Then, the scale factor was 0.9804.[15]

Results and Discussion

^{1}H NMR from BMTP. Figure 2 shows methine and methylene parts of ^{1}H NMR spectra observed from BMTP (a) in C_6D_6 at 26 °C and (b) in the gas phase at 150 °C. In previous studies,[18,19] ^{1}H NMR chemical shifts of isotactic PPS were assigned to the methine and methylene protons by comparison with those of poly(propene-2-d_1 sulfide) $[CH_2C^*D(CH_3)S]_x$. Following the assignment, we simulated the ^{1}H NMR spectra of BMTP. The calculated spectra are also shown in Figure 2. Vicinal coupling constants, $^3J_{AC}$ and $^3J_{BC}$, were respectively determined as 4.40 and 9.57 Hz (C_6D_6) and 3.8 ± 0.4 and 10.0 ± 0.4 Hz (gas phase). All spectra observed from three solutions at different temperatures were satisfactorily reproduced, and the $^3J_{AC}$ and $^3J_{BC}$ values were obtained as listed in Table 1.

Trans and gauche$^\pm$ states around the C–C* bond of BMTP are depicted in Figure 3b. With the rotational isomeric state (RIS) approximation, the observed vicinal $^1H-^1H$ coupling constants, $^3J_{AC}$ and $^3J_{BC}$, can be expressed as

$$^3J_{AC} = {}^3J_G^{HH} + ({}^3J_T^{HH} - {}^3J_G^{HH})p_{g+}^{CC*} \tag{1}$$

and

$$^3J_{BC} = {}^3J_G^{HH} + ({}^3J_T^{HH} - {}^3J_G^{HH})p_{t}^{CC*} \tag{2}$$

where $^3J_T^{HH}$ and $^3J_G^{HH}$ are respectively vicinal coupling constants between protons in the trans and gauche positions and p_t^{CC*} and p_{g+}^{CC*} are trans and gauche$^+$ fractions of the C–C* bond, respectively. The definition of the bond conformations dictates that

$$p_t^{CC*} + p_{g+}^{CC*} + p_{g-}^{CC*} = 1 \tag{3}$$

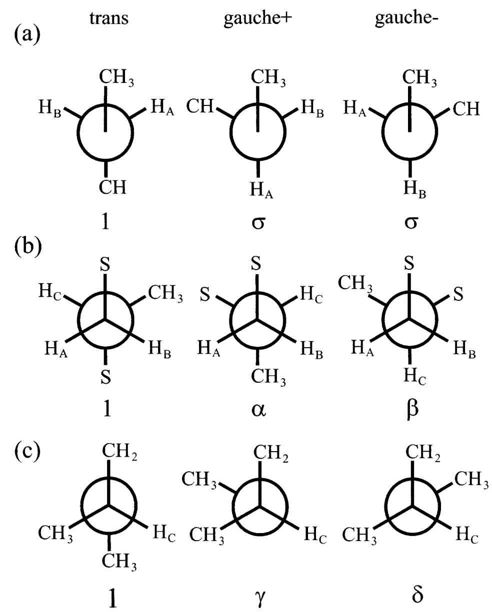

Figure 3. Rotational isomeric states around (a) bonds 2 and a, (b) bonds 3 and b, and (c) bonds 4 and c of BMTP and isotactic PPS. The first-order intramolecular interactions are represented by the statistical weights.

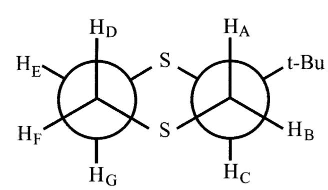

Figure 4. (a) 2-(1,1-Dimethylethyl)-1,4-dithiane (DMEDT). The proton atoms are designated as indicated.

To obtain the p_t^{CC*}, p_{g+}^{CC*}, and p_{g-}^{CC*} values from eqs 1–3, the $^3J_T^{HH}$ and $^3J_G^{HH}$ values must be given. In our previous[2] and present studies, their values for S–C–C–S bond sequences were derived from a cyclic compound, DMEDT (see Figure 4; observed and calculated spectra for the C_6D_{12} solution at 25.0 °C are shown in Figure 2c). All vicinal coupling constants of DMEDT in C_6D_6 and $CDCl_3$ were already reported,[2] and those of DMEDT in C_6D_{12} are given in Table 2. The bulky *tert*-butyl group prevents the DMEDT ring from changing the conformation, and hence the temperature depen-

Table 2. Observed Vicinal ^{1}H−^{1}H Coupling Constants[a] of DMEDT[b] in Cyclohexane-d_{12}

temp (°C)	$^3J_{AC}$	$^3J_{DG}$	$^3J_{BC}$	$^3J_{DE}$	$^3J_{EF}$	$^3J_{FG}$	$^3J_T^{HH}$ [c]	$^3J_G^{HH}$ [d]
15.0	10.82	12.06	1.90	2.40	4.11	2.42	11.44	2.98
25.0	10.85	12.04	1.85	2.41	4.12	2.44	11.45	2.99
35.0	10.73	12.08	2.01	2.40	4.13	2.43	11.41	2.99
55.0	10.83	11.96	1.81	2.43	4.18	2.45	11.40	3.02
70.0	10.90	11.93	1.84	2.44	4.18	2.50	11.42	3.04

[a] In Hz. [b] For designation of protons, see Figure 4. [c] $^3J_T{}^{HH} = (^3J_{AC} + {}^3J_{DG})/2$. [d] $^3J_G{}^{HH} = (^3J_{DE} + {}^3J_{EF} + {}^3J_{FG})/3$. Dihedral angles ($\phi$'s) of DMEDT were obtained by MO calculations at the B3LYP/6-31G(d) level: $\phi_{AC} = 172.37°$, $\phi_{DG} = 178.79°$, $\phi_{BC} = 67.94°$, $\phi_{DE} = 59.54°$, $\phi_{EF} = 59.86°$, and $\phi_{FG} = 59.39°$. Since ϕ_{BC} somewhat deviates from 60°, $^3J_{BC}$ was not employed to calculate $^3J_G{}^{HH}$'s. Note that ϕ's here are defined differently from those used in the RIS calculations (Table 6).

dence of ^3J's is negligible. The $^3J_T^{HH}$ and $^3J_G^{HH}$ values were determined by an average over temperatures for each solution: $^3J_T^{HH} = 11.42$ Hz and $^3J_G^{HH} = 3.00$ Hz (obtained from the C_6D_{12} solution of DMEDT and used for the gas phase and C_6D_{12} solution of BMTP); $^3J_T^{HH} = 11.42$ Hz and $^3J_G^{HH} = 2.98$ Hz (from the C_6D_6 solution of DMEDT and for the C_6D_6 solution of BMTP); $^3J_T^{HH} = 11.48$ Hz and $^3J_G^{HH} = 3.01$ Hz (from the $CDCl_3$ solution of DMEDT and for the DMSO solution of BMTP). The bond conformations derived therefrom are shown in Table 3. From the table, it can be seen that p_t^{CC*} decreases and p_{g+}^{CC*} increases with temperature and polarity of solvent.

^{13}C NMR from BMTP. Figure 5 shows ^{13}C NMR spectra observed from two methoxy carbons of BMTP in C_6D_6 at 26 °C. Both signals are largely split into four by direct couplings with the methoxy protons. The signal of carbon 1 is further divided into four by protons A and B and that of carbon 6 into two by proton C. The peak spacings directly give vicinal coupling constants, $^3J_{CHA}$, $^3J_{CHB}$, and $^3J_{CHC}$. The two ^3J values of carbon 1 were assigned to $^3J_{CHA}$ and $^3J_{CHB}$ on the basis of MO calculations to be shown later; p_{g-}^{SC} would be larger than p_{g+}^{SC}, where p_{g+}^{SC} and p_{g-}^{SC} are gauche$^+$ and gauche$^-$ fractions of bond 2. The $^3J_{CH}$ values for the C_6D_{12}, C_6D_6, and DMSO solutions at different temperatures are given in Table 1.

The observed $^3J_{CHA}$ and $^3J_{CHB}$ values may be expressed as

$$^3J_{CHA} = {}^3J_G^{CH} + ({}^3J_T^{CH} - {}^3J_G^{CH})p_{g+}^{SC} \tag{4}$$

and

$$^3J_{CHB} = {}^3J_G^{CH} + ({}^3J_T^{CH} - {}^3J_G^{CH})p_{g-}^{SC} \tag{5}$$

where $^3J_G^{CH}$ and $^3J_T^{CH}$ are vicinal coupling constants between carbon and proton in trans and gauche posi-

Table 3. Bond Conformations of BMTE and Isotactic PPS

	medium	temp (°C)	2 (a) p_t^{SC}	2 (a) p_{g+}^{SC}	2 (a) p_{g-}^{SC}	3 (b) p_t^{CC*}	3 (b) p_{g+}^{CC*}	3 (b) p_{g-}^{CC*}	4 (c) p_t^{C*S}	4 (c) p_{g+}^{C*S}	4 (c) p_{g-}^{C*S}
BMTP											
					NMR						
	gas	150				0.83 ± 0.05	0.10 ± 0.05	0.07 ± 0.05			
	cyclohexane	10.0	0.03	0.34	0.63	0.86	0.11	0.03		0.21	
		26.0	0.04	0.34	0.62	0.83	0.13	0.04		0.22	
		43.0	0.05	0.35	0.60	0.81	0.14	0.05		0.22	
		59.0	0.06	0.35	0.59	0.79	0.15	0.06		0.23	
		75.0	0.07	0.35	0.58	0.77	0.16	0.07		0.23	
	benzene	10.0	0.10	0.32	0.58	0.80	0.16	0.04		0.20	
		26.0	0.10	0.32	0.58	0.78	0.17	0.05		0.20	
		43.0	0.11	0.33	0.56	0.76	0.19	0.05		0.20	
		59.0	0.12	0.33	0.55	0.76	0.18	0.06		0.20	
		75.0	0.13	0.33	0.54	0.72	0.19	0.09		0.20	
	DMSO	25.0	0.12	0.31	0.57	0.72	0.20	0.08		0.14	
		41.0	0.12	0.32	0.56	0.71	0.21	0.08		0.16	
		58.0	0.13	0.32	0.55	0.69	0.23	0.08		0.16	
		74.0	0.13	0.33	0.54	0.68	0.23	0.09		0.18	
		90.0	0.14	0.34	0.52	0.67	0.23	0.10		0.18	
					Ab Initio MO						
	gas (MP2[a])	25.0	0.24	0.16	0.60	0.82	0.11	0.07	0.26	0.17	0.57
		150[b]	0.29	0.22	0.49	0.70	0.18	0.12	0.29	0.21	0.50
	gas (B3LYP[c])	25.0	0.29	0.09	0.62	0.92	0.06	0.02	0.26	0.11	0.63
		150[b]	0.32	0.14	0.54	0.84	0.11	0.05	0.30	0.15	0.55
					RIS Simulation						
	set I[d]	26.0	0.12	0.39	0.49	0.77	0.18	0.05	0.52	0.20	0.28
	set II[d]	26.0	0.20	0.36	0.44	0.77	0.18	0.05	0.52	0.22	0.26
isotactic PPS											
					NMR[e]						
	CCl_4	17				0.71	0.21	0.08			
					RIS Simulation						
	set I	26.0	0.17	0.36	0.47	0.77	0.19	0.04	0.59	0.12	0.29
	set II	26.0	0.29	0.31	0.40	0.76	0.20	0.04	0.59	0.15	0.26

[a] At the MP2/6-311+G(3df, 2p)//HF/6-31G(d) level. [b] Calculated from conformer free energies of BMPT at 150 °C and 7.1 atm and at 150 °C and 1.0 atm (not shown). The difference in pressure had essentially no effect on the bond conformations. [c] At the B3LYP/6-311+G(3df, 2p)//HF/6-31G(d) level. [d] Bond conformations at other temperatures were also reproduced fairly well. [e] Calculated from $^3J_{AC} = 4.8$ Hz and $^3J_{BC} = 9.0$ Hz.[31]

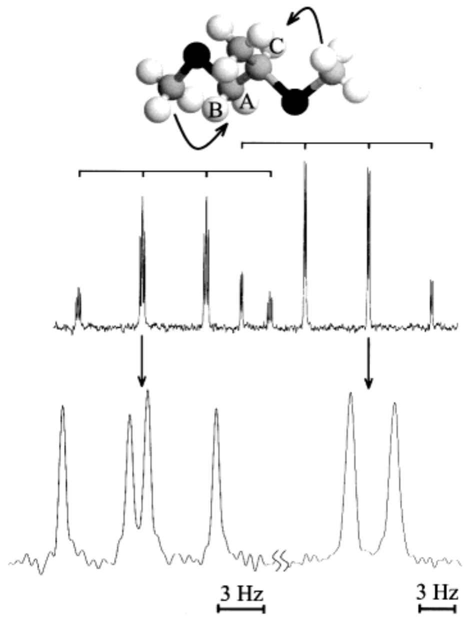

Figure 5. ^{13}C NMR spectra observed from methoxy carbons of BMTP in C_6D_6 at 26 °C.

tions, respectively. From the definition of p_{η}^{SC}'s (η = t, g$^+$, or g$^-$), we have

$$p_{t}^{SC} + p_{g+}^{SC} + p_{g-}^{SC} = 1 \qquad (6)$$

These bond conformations can be determined from observed $^3J_{CHA}$ and $^3J_{CHB}$ values, provided that $^3J_{G}^{CH}$ and $^3J_{T}^{CH}$ are given. The $^3J_{CHC}$ value is expressed as

$$^3J_{CHC} = {}^3J_{G}^{CH} + ({}^3J_{T}^{CH} - {}^3J_{G}^{CH})p_{g+}^{C*S} \qquad (7)$$

where p_{g+}^{C*S} is the gauche$^+$ fraction of bond 4. Equation 7 yields the p_{g+}^{C*S} value, whereas the trans and gauche$^-$ fractions (p_{t}^{C*S} and p_{g-}^{C*S}) remain indeterminate.

The $^3J_{G}^{CH}$ and $^3J_{T}^{CH}$ values obtained from 2-methyl-1,3,5-trithiane,[1] which has the C−S−C−H bond sequence, were employed here: $^3J_{T}^{CH}$ = 7.13 Hz and $^3J_{G}^{CH}$ = 2.62 Hz (for the C_6D_{12} and C_6D_6 solutions); $^3J_{T}^{CH}$ = 6.92 Hz and $^3J_{G}^{CH}$ = 2.71 Hz (for the DMSO solution). The p_{t}^{SC}, p_{g+}^{SC}, p_{g-}^{SC}, and p_{g+}^{C*S} values thus evaluated are listed in Table 3. It can be seen that p_{t}^{SC} increases and p_{g+}^{C*S} decreases with increasing polarity of solvent.

Free Energies, Bond Conformations, and Conformational Energies of BMTP, Obtained from MO Calculations. Free energies (ΔG_k's) of conformers of BMTP at 25 °C and 1.0 atm, obtained from the ab initio MO calculations, are listed in Table 4. The bond conformations, evaluated from ΔG_k's with eq 11 of paper I, are shown in Table 3. The ΔG_k values at 150 °C and 7.1 atm and at 150 °C and 1.0 atm were also calculated. However, the two sets of free energies were coincident with each other to the second decimal place (in kcal mol^{-1}); that is, no particular pressure dependence was found in the free energies and bond conformations within this pressure range.

Analogous to statistical weight matrices ($\mathbf{U}_i$'s, *i*: bond number) of 1,2-dimethoxypropane (DMP, $CH_3OCH_2C^*H(CH_3)OCH_3$), a monomeric model compound of poly(propylene oxide) (PPO), those of BMTP were formulated according to the 9 × 9 matrix scheme.[20−22] The statistical weights are designated so as to correspond to those of DMP and PPO[23,24] (see Figures 3 and 6). The statistical weight is related to the corresponding conformational energy through the Boltzmann factor; for example, $\alpha = \exp(-E_\alpha/RT)$, where R is the gas constant and T is the absolute temperature. The geometrical optimization by the MO calculations gave only 19 conformers for DMP[23] but as many as 25 conformers for BMTP (Table 4). This may be due to the difference between the C−O and C−S bond lengths. Accordingly, two statistical weights (τ and ζ) representing second-order interactions have been introduced to $\mathbf{U}_i$'s of BMTP and PPS. For DMP and PPO, on the other hand, these parameters were assumed to be null; that is, $E_\tau = E_\zeta = \infty$. Visual inspection of the molecular model and the above consideration led to the following statistical weight matrices for BMTP:

Table 4. Free Energies (ΔG_k's) Dipole Moments (μ_k's) of Conformers of BMTP, Evaluated by ab Initio Molecular Orbital Calculations

			ΔG_k[a] (kcal mol^{-1})		μ_k (D)	
k	conformation	statistical weight[b]	MP2[c]	B3LYP[d]	MO[d]	BOND[e]
1	ttt	1	0.00	0.00	0.35	0.41
2	ttg$^+$	γ	0.42	0.60	1.93	2.17
3	ttg$^-$	δ	−0.46	−0.61	1.73	2.08
4	tg$^+$t	α	0.81	1.17	2.31	2.25
5	tg$^+$g$^+$	$\alpha\gamma$	0.89	1.76	2.90	3.07
6	tg$^+$g$^-$	$\alpha\delta\omega_1$	0.99	1.44	1.77	1.88
7	tg$^-$t	β	1.20	1.71	2.47	2.40
8	tg$^-$g$^+$	$\beta\gamma\omega_2$	2.15	2.75	1.71	1.78
9	tg$^-$g$^-$	$\beta\delta$	0.72	1.65	2.82	3.11
10	g$^+$tt	$\sigma\tau$	0.63	0.82	1.70	1.52
11	g$^+$tg$^+$	$\sigma\gamma\tau$	1.05	1.49	2.55	2.58
12	g$^+$tg$^-$	$\sigma\delta\tau$	0.14	0.42	0.41	0.61
13	g$^+$g$^+$t	$\sigma\alpha$	0.83	1.28	3.02	2.92
14	g$^+$g$^+$g$^+$	$\sigma\alpha\gamma\chi$	0.99	2.34	1.73	1.60
15	g$^+$g$^+$g$^-$	$\sigma\alpha\delta\omega_1$	0.78	1.46	2.48	2.46
16	g$^+$g$^-$t	$\sigma\beta\omega_2$	0.81	1.70	1.96	1.62
17	g$^+$g$^-$g$^+$[f]					
18	g$^+$g$^-$g$^-$	$\sigma\beta\delta\omega_2$	0.72	1.73	2.28	2.31
19	g$^-$tt	σ	−0.55	−0.54	2.02	1.99
20	g$^-$tg$^+$	$\sigma\gamma$	−0.25	0.11	0.19	0.38
21	g$^-$tg$^-$	$\sigma\delta$	−0.96	−0.84	2.20	2.31
22	g$^-$g$^+$t	$\sigma\alpha\omega_1$	0.71	1.16	1.56	1.08
23	g$^-$g$^+$g$^+$	$\sigma\alpha\gamma\omega_1$	1.33	2.02	2.45	2.29
24	g$^-$g$^+$g$^-$[f]					
25	g$^-$g$^-$t	$\sigma\beta\tau$	1.91	2.28	3.03	2.84
26	g$^-$g$^-$g$^+$	$\sigma\beta\gamma\tau\omega_2$	2.75	3.59	2.52	2.35
27	g$^-$g$^-$g$^-$	$\sigma\beta\delta\tau$	1.39	2.26	2.65	2.61

[a] Relative to the ΔG_k value of the all-trans conformation. At 25 °C and 1 atm. [b] For definition of the statistical weights, see Figures 3 and 6. [c] At the MP2/6-311+G(3df, 2p)//HF/6-31G(d) level. [d] At the B3LYP/6-311+G(3df, 2p)//B3LYP/6-31G(d) level. [e] Evaluated from bond dipole moments: $m_{S-C} = m_{C^*-S} = 1.21$ D and $m_{C-C^*} = 0.00$ D. [f] These cyclic conformers were considered to be absent.

$$\mathbf{U}_2 = \begin{bmatrix} 1 & \sigma & \sigma \\ 0 & 0 & 0 \\ 0 & 0 & 0 \end{bmatrix} \qquad (8)$$

$$\mathbf{U}_3 = \begin{bmatrix} 1 & \alpha & \beta & 0 & 0 & 0 & 0 & 0 & 0 \\ 0 & 0 & 0 & \tau & \alpha & \beta\omega_2 & 0 & 0 & 0 \\ 0 & 0 & 0 & 0 & 0 & 0 & 1 & \alpha\omega_1 & \beta\tau \end{bmatrix} \qquad (9)$$

and

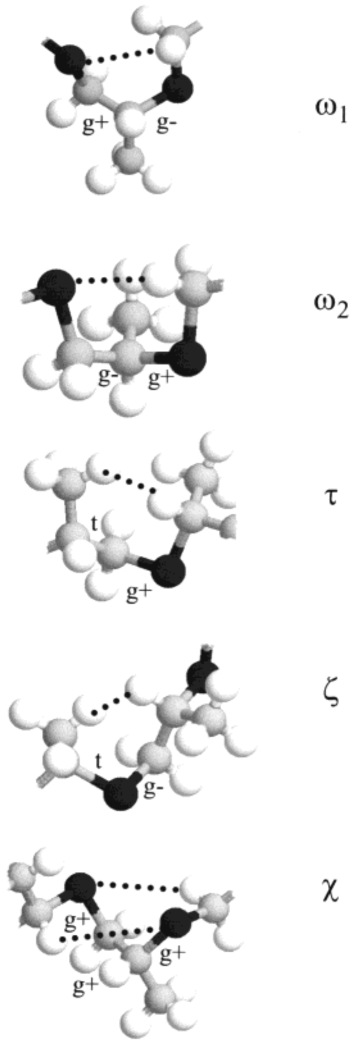

Figure 6. Second-order ω_1, ω_2, τ, and ζ and third-order χ interactions defined for BMTP and PPS.

$$\mathbf{U}_4 = \begin{bmatrix} 1 & \gamma & \delta & 0 & 0 & 0 & 0 & 0 & 0 \\ 0 & 0 & 0 & 1 & \gamma & \delta\omega_1 & 0 & 0 & 0 \\ 0 & 0 & 0 & 0 & 0 & 0 & 1 & \gamma\omega_2 & \delta \\ 1 & \gamma & \delta & 0 & 0 & 0 & 0 & 0 & 0 \\ 0 & 0 & 0 & 1 & \gamma\chi & \delta\omega_1 & 0 & 0 & 0 \\ 0 & 0 & 0 & 0 & 0 & 0 & 1 & 0 & \delta \\ 1 & \gamma & \delta & 0 & 0 & 0 & 0 & 0 & 0 \\ 0 & 0 & 0 & 1 & \gamma & 0 & 0 & 0 & 0 \\ 0 & 0 & 0 & 0 & 0 & 0 & 1 & \gamma\omega_2 & \delta \end{bmatrix} \qquad (10)$$

Similarly, the $\mathbf{U}_i$ matrices corresponding to four linkage types ($R \rightarrow R$, $R \rightarrow S$, $S \rightarrow S$, and $S \rightarrow R$) of atactic PPS were derived as shown in the Appendix.

In the RIS scheme,[20,21] the conformer free energy of BMTP is represented as a function of E_ξ's ($\xi = \alpha, \beta, \gamma, \delta, \sigma, \omega_1, \omega_2, \tau, \zeta$, and χ). For example, the $g^+g^+g^+$ conformation has a weight of $\sigma\alpha\gamma\chi$. Thus, the ΔG_k value may be approximated by $E_\sigma + E_\alpha + E_\gamma + E_\chi$. The E_ξ values were determined by minimizing the standard deviation between ΔG_k's and sums of E_ξ's of the conformers (eqs 15 and 16 of paper I). The temperature T was set to 298.15 K. The conformational energies thus evaluated are shown in Table 5.

Bond Dipole Moments. The bond dipole moment (m_{S-C}) of the S−C bond was estimated from the MO

Table 5. Conformational Energies[a] and Configurational Entropies (S_{conf}'s) of PPS (BMTP), PES, and PPO

	BMTP and PPS				PES	PPO
	MO		exptl		exptl	exptl
	MP2[b]	B3LYP[c]	set I[d]	set II[e]	benzene[f]	benzene[g]
First-Order Interaction						
E_α	0.93	1.38	0.55	0.49	0.41	0.54
E_β	1.19	1.85	1.13	1.18		0.83
E_γ	0.30	0.55	0.49	0.43		2.97
E_δ	−0.43	−0.48	0.25	0.27		0.22
E_σ	−0.52	−0.43	−0.99	−0.60	−0.74	1.41
Second-Order Interaction						
E_{ω_1}	0.55	0.51	0.64	0.89	0.40	−1.04
E_{ω_2}	0.35	0.51	1.16	0.99		−1.75
E_τ	1.14	1.30	0.26	0.28		∞
E_ζ[h]			0.35	0.35		∞
Third-Order Interaction						
E_χ	0.29	0.84	0.38	0.42	0.46	−0.91
S_{conf}[i] (cal mol^{-1} K^{-1})			4.3	4.6	6.2	4.0

[a] In kcal mol^{-1}. [b] At the MP2/6-311+G(3df, 2p)//HF/6-31G(d) level. [c] At the B3LYP/6-311+G(3df, 2p)//B3LYP/6-31G(d) level. [d] Determined from bond conformations of BMTP in benzene at 10, 26, 43, 59, and 75 °C (Table 3) and dipole moment ratios of isotactic and atactic PPS in benzene at 25 °C (Table 7). [e] Determined from the bond conformations, the dipole moment ratios, and the characteristic ratio of atactic PPS in the Θ solvent (*n*-hexane (31%) and toluene) (Table 7). [f] Reference 2. [g] Determined for isotactic PPO in benzene.[23,24] [h] To evaluate the E_ζ value by MO calculations, the geometrical optimizations at the HF/6-31G(d) and B3LYP/6-31G(d) levels were carried out for the tttg$^-$tt conformation of an *RR* dimeric model compound, $CH_3S-CH_2-C^*H(CH_3)-S-CH_2-C^*H(CH_3)-SCH_3$ because the E_ζ value may be estimated from the energy difference ($=E_\sigma + E_\zeta$) between the tttg$^-$tt and tttttt states. However, the local minimum was not found. On the other hand, the MM2 calculations gave the potential minimum. In the RIS simulations, the E_ζ value was initially set to null. [i] At the individual melting points: 53 °C (PPS), 216 °C (PES), and 73 °C (PPO).

calculations on BMTP; the m_{S-C} value was optimized so as to minimize the difference between μ_k^{MO}'s and μ_k^{BOND}'s (eqs 17 and 18 of paper I), where μ_k^{MO} is the dipole moment of conformer k of BMTP, obtained from the MO calculations, and μ_k^{BOND} is that calculated as the sum of the bond dipole moment vectors. Then, we employed ΔG_k's at the MP2/6-311+G(3df, 2p) level and μ_k^{MO}'s at the B3LYP/6-311+G(3df, 2p) level because this combination yielded the best results for 1,2-bis(methylthio)ethane, a monomeric model compound of PES.[2] It was assumed that that $m_{S-C} = m_{C^*-S}$ and $m_{C-C^*} = 0$. Consequently, μ_k^{BOND}'s agreed well with μ_k^{MO}'s, as shown in Table 4; the standard deviation between μ_k^{MO}'s and μ_k^{BOND}'s was minimized to 0.14. The m_{S-C} value was obtained as 1.21 D, being in agreement with that used by Riande et al.,[11,12] Riande and Siaz,[25] and Abe[7,26] for polysulfides and close to those optimized by us for PMS (1.23 D)[1] and PES (1.22 D).[2]

Synthesis of Atactic PPS Chain in Computer. Statistical weight matrices for bonds a, b, and c of isotactic (*R*)-PPS may be given by eqs A1, A2, and A3 (Appendix). The atactic chain was synthesized and its configuration-dependent properties were calculated according to the following procedures: (1) A number is sampled out of a set, in which numbers are distributed uniformly between zero and unity (random-number generation). (2) If the number is smaller than or equal

Table 6. Geometrical Parameters Used in RIS Simulations for Isotactic and Atactic PPS

Bond Length[a] (Å)	
C−S	1.818
C−C*	1.529
Bond Angle[a] (deg)	
CSC	101.60
SCC*	114.59
CC*S	110.23
Dihedral Angle[b] (deg)	
bond a	
t	−2.55
g+	89.09
g−	−101.10
bond b	
t	10.32
g+	112.40
g−	−114.58
bond c	
t	−12.87
g+	113.96
g−	−105.60
Bond Dipole Moment (D)	
S−C	1.21
C*−C	0.00
C*−S	1.21

[a] From the all-trans conformation of BMTP. At the HF/6-31G(d) level. [b] Evaluated from $\langle\phi_\eta\rangle = \sum_{k_\eta}\phi_{k_\eta}\exp(-\Delta G_{k_\eta}/RT)/\sum_{k_\eta}\exp(-\Delta G_{k_\eta}/RT)$, where $\langle\phi_\eta\rangle$ is the weight-average dihedral angle of the η (= t, g^+, or g^-) state and ϕ_{k_η} and ΔG_{k_η} are the dihedral angle and free energy of conformer k_η (of BMTP), which has the η conformation in the bond of interest.

to a given value of (R)-monomer fraction in a chain, P_R, an (R)-unit is added to the propagating end of the polymeric chain. Otherwise, an (S)-unit is added. (3) Statistical weight matrices (Appendix) corresponding to the linkage type formed ($R \rightarrow R$, $R \rightarrow S$, $S \rightarrow S$, or $S \rightarrow R$, see Figure 1c) are chosen. The procedures 1−3 are repeated up to a given degree of polymerization. (4) From a series of statistical weight matrices thus arranged, the characteristic ratio $\langle r^2\rangle_0/nl^2$ and dipole moment ratio $\langle\mu^2\rangle/nm^2$ are calculated, where r is the end-to-end distance, n is the number of skeletal bonds, l is the bond length, μ is the dipole moment, m is the bond dipole moment, the angular brackets represent the ensemble average, and the subscript 0 stands for the unperturbed state.

Conformational Energies and Configuration-Dependent Properties of PPS. Conformational energies of PPS were attempted to be determined by RIS simulations for experimental observations of the following configuration-dependent properties: simulation I, bond conformations of BMTP in benzene at 10, 26, 43, 59, and 75 °C and dipole moment ratios[11] of isotactic and atactic PPS; simulation II, the characteristic ratio[10] of atactic PPS in the Θ solvent (n-heptane (31%) and toluene) as well as the experimental data used in simulation I. The 10 energy parameters E_ξ's were optimized by the Simplex method[27] for 37 (simulation I) or 38 (simulation II) experimental data. Then, the conformational energies at the MP2 level were employed as the initial values. Geometrical parameters used are shown in Table 6. For both isotactic and atactic chains, the degree of polymerization, x, was set to 200. For the atactic chain, P_R was set to 0.5, and 100 chains were generated; the $\langle r^2\rangle_0/nl^2$ and $\langle\mu^2\rangle/nm^2$ values were averaged over the 100 chains. The E_ξ values determined in simulations I and II, designated as sets I and II, respectively, are listed in Table 5. The bond conformations of BMTP and isotactic PPS at 26 °C, calculated from the two sets of energy parameters, are given in Table 3. In Table 7, the calculated $\langle r^2\rangle_0/nl^2$ and $\langle\mu^2\rangle/nm^2$ values and their temperature coefficients, 10^3 d ln $\langle r^2\rangle_0$/dT and 10^3 d ln $\langle\mu^2\rangle$/dT, are compared with the corresponding experimental data.

The bond conformations of BMTP and dipole moment ratios and the temperature coefficients of isotactic and atactic PPS were satisfactorily reproduced by simulation I. However, the characteristic ratio of the atactic chain was calculated to be 3.2, being smaller than that (4.0) observed from the Θ solution.[10] On the other hand, simulation II gave better agreement between the calculated and observed $\langle r^2\rangle_0/nl^2$ and $\langle\mu^2\rangle/nm^2$ values but moderate agreement for bond conformations of BMTP. The 10^3 d ln $\langle r^2\rangle_0$/dT value estimated from thermoelasticity measurements on networks of atactic PPS is positive, 0.51 ± 0.11,[28,29] close to that (0.87) obtained in simulation II. However, the temperature coefficients obtained from the monomer (cyclic propylene sulfide) solution are negative: −2.8 ± 0.3 (isotactic) and −2.0 ± 0.3 (atactic).[30] The $^3J_{AC}$ and $^3J_{BC}$ values of isotactic PPS in CCl_4 at 17 °C were estimated as 4.8 and 9.0 Hz, respectively.[31] From these values and $^3J_T^{HH} = 11.48$ and $^3J_G^{HH} = 3.01$ Hz, we can derive $p_t^{CC*} = 0.71$, $p_{g+}^{CC*} = 0.21$, and $p_{g-}^{CC*} = 0.08$, which are close to those calculated from the energy parameters of sets I and II (see Table 3).

Conformational energies of PES, determined for the benzene solution,[2] are also shown in Table 5. The first-

Table 7. Configuration-Dependent Properties of PPS[a]

	isotactic			atactic		
	calcd			calcd		
	set I	set II	obsd	set I	set II	obsd
$\langle r^2\rangle_0/nl^2$	3.3	4.0		3.2	3.9	4.0[b]
10^3 d ln $\langle r^2\rangle_0$/dT, K^{-1}	1.0	0.47	−2.8 ± 0.3[c]	1.6	0.87	−2.0 ± 0.3[c] 0.51 ± 0.11[d]
$\langle\mu^2\rangle/nm^2$	0.33	0.34	0.33[e] (CCl_4) 0.39[e] (C_6H_6)	0.38	0.38	0.37[e] 0.36[f] (CCl_4) 0.44[e] 0.44[f] (C_6H_6)
10^3 d ln $\langle\mu^2\rangle$/dT, K^{-1}	2.2	2.3	2.1[e] (CCl_4) 2.0[e] (C_6H_6)	2.9	2.6	4.0[e] 2.8[f] (CCl_4) 1.5[e] 0.72[f] (C_6H_6)

[a] At 25 °C. [b] Rescaled with $l_{C-S} = 1.818$ Å and $l_{C-C} = 1.529$ Å. Evaluated from the intrinsic viscosity of atactic PPS in the Θ solvent of n-heptane (31%) and toluene at 25 °C.[10] [c] Obtained from the intrinsic viscosity of PPS in the monomer, cyclic propylene sulfide.[30] [d] Estimated from thermoelasticity measurements on networks of atactic PPS.[28,29] [e] From isotactic PPS of the weight-average molecular weight = 1.6 × 10^6 and atactic PPS of the weight-average molecular weight = 5 × 10^5.[11] [f] From atactic PPS of the number-average molecular weight = 5−6 × 10^3.[12]

Table 8. First Derivatives of Characteristic Ratios and Dipole Moment Ratios of Isotactic and Atactic PPS with Respect to Conformational Energies (E_ξ's) of Set II

	$\partial(\langle r^2\rangle_0/nl^2)/\partial E_\xi$		$\partial(\langle \mu^2\rangle/nm^2)/\partial E_\xi$	
ξ	isotactic	atactic	isotactic	atactic
	First-Order Interaction			
α	0.14	−0.03	−0.38	−0.36
β	−0.16	−0.23	−0.08	−0.11
γ	0.25	−0.20	0.02	−0.02
δ	1.53	0.92	0.10	0.08
σ	2.06	1.86	−0.02	−0.03
	Second-Order Interaction			
ω_1	0.30	0.24	−0.03	−0.04
ω_2	0.04	0.04	−0.01	−0.01
τ	−0.70	−0.54	0.10	0.05
ζ	0.55	0.49	0.03	−0.08
	Third-Order Interaction			
χ	−0.08	−0.10	−0.03	−0.04

order interaction energies for the C−S and C−C bond of PES are respectively −0.74 and +0.41 kcal mol^{-1}, thus being comparable to those of PPS. On the other hand, the $E_{\omega 1}$ and $E_{\omega 2}$ values, representing C−H···S close contacts, are larger than E_ω of PES because the steric repulsions may be raised by the methyl side chain. The MO calculations on BMTP estimated E_α and E_τ to be larger and E_δ, $E_{\omega 1}$, and $E_{\omega 2}$ to be smaller than the corresponding experimental values. The MO data reflect the gas-phase structure. Therefore, these differences may be partly due to solvent effects, being much larger than those found for PMS[1] and PES.[2]

In Table 5, conformational energies of PPO in benzene[23,24] are also shown. Interestingly, both E_α and E_β of PPO are comparable to those of PPS. As shown above, the C−C* bond of PPS strongly prefers the trans state, whereas that of isotactic (*R*)-PPO exhibits a gauche$^+$ preference[23] (the gauche-oxygen effect).[32] This is obviously due to the difference in signs of $E_{\omega 1}$ and $E_{\omega 2}$; the intramolecular (C−H)···O interactions of PPO are attractive, while the C−H···S interactions of PPS are repulsive. As found for PES, the S−CH_2 bond of PPS also shows a gauche preference. In the C*−S bond, however, the trans state is the most stable. The C*−S and S−C bonds, being longer than C*−O and O−C, reduce steric repulsions occurring in the g$^+$ state of the C*−S bond: E_γ (PPS) = 0.43−0.49 and E_γ (PPO) = 2.97 kcal mol^{-1}. The conformational preferences of PPS are, in general, similar to those of PES but different from those of PPO.

The configurational entropy S_{conf} of $x = 200$ of isotactic PPS at the melting point of 53 °C was calculated according to the conventional method.[33−36] The S_{conf} value was obtained as 4.3 (set I) and 4.6 (set II) cal mol^{-1} K^{-1}, being close to that (4.0) of PPO but smaller than that (6.2) of PES[2] (Table 5). Melting points of PPO and PES are 73 and 216 °C, respectively. These data indicate that crystallized PES has much stronger intermolecular interactions than PPS. Interestingly, isotactic PPS and PPO form isomorphic crystals,[4] although their conformational characteristics in the Θ state are significantly different from each other.

Solvent Effects. To investigate the dependence of the chain dimension and dipole moment on the conformational energies, the first derivatives, $\partial(\langle r^2\rangle_0/nl^2)/\partial E_\xi$ and $\partial(\langle \mu^2\rangle/nm^2)/\partial E_\xi$, were estimated (Table 8). The data show that the $\langle r^2\rangle_0/nl^2$ and $\langle \mu^2\rangle/nm^2$ values are sensitive to changes in first-order interaction energies for the S−C (C*−S) and C−C bonds, respectively. A comparatively large difference between sets I and II can be seen in E_σ: set I, −0.99 kcal mol^{-1}; set II, −0.60 kcal mol^{-1}. Conformational energies of the S−C bonds of PMS and PES were found to vary with solvent.[1,2] If E_σ and E_δ are respectively changed to 0.0 and 0.4 kcal mol^{-1} with other energies fixed at the set II parameters, the 10^3 d ln $\langle r^2\rangle_0$/dT values of isotactic and atactic PPS are reduced to −1.1 and −0.5, respectively. If other energy parameters are also adjusted slightly, the negative temperature coefficients[30] can be more closely reproduced, whereas the bond conformations of BMTP become far from satisfactory.

In a previous study,[26] Abe estimated the conformational energies of PPS so as to reproduce experimental $\langle r^2\rangle_0/nl^2$ and $\langle \mu^2\rangle/nm^2$ values and their temperature coefficients. Then, the energy parameters of E_γ, E_δ, $E_{\omega 1}$, $E_{\omega 2}$, E_τ, and E_ζ were treated as constants, of which the values were calculated from semiempirical potential functions; accordingly, only E_α, E_β, and E_σ were adjusted (E_χ was not defined). The results are as follows: E_α = 0.33, E_β = 1.3, E_γ = 1.2, E_δ = 0.1, E_σ = −0.05, $E_{\omega 1}$ = $E_{\omega 2}$ = 1.1, E_τ = 1.5, and E_ζ = 0.4 kcal mol^{-1}. The first-order interaction energies, E_α and E_β, for the C−C* bond agree well with our values. The E_σ value, being larger than ours, would be required to reach the experimental $\langle r^2\rangle_0/nl^2$ value and yield negative 10^3 d ln $\langle r^2\rangle_0$/dT values.

Nagai and Ishikawa[37] and Doi[38] theoretically examined the relationship between the excluded volume effect and dipole moment of polymers and derived an equation

$$\alpha_u^{\ 2} - 1 = \frac{\langle \vec{r}\cdot\vec{\mu}\rangle_0^{\ 2}}{\langle r^2\rangle_0 \langle \mu^2\rangle_0} (\alpha_r^{\ 2} - 1) \tag{11}$$

where $\alpha_u^{\ 2} = \langle \mu^2\rangle/\langle \mu^2\rangle_0$, $\alpha_r^{\ 2} = \langle r^2\rangle/\langle r^2\rangle_0$, $\vec{r}$ is the end-to-end vector, and $\vec{\mu}$ is the dipole moment vector. If $\langle \vec{r}\cdot\vec{\mu}\rangle_0^2 = 0$, the dipole moment is free from the excluded volume effect. Polymers such as PEO and PES, possessing a mirror plane, a 2-fold axis of symmetry, or a center of symmetry between adjoining repeating units in the all-trans conformation, satisfy the above condition. Since PPS lacks these symmetries owing to the methyl side chain, the dipole moments may be affected by the excluded volume effect. Riande et al.[11,12] pointed out the possibility that the large differences in $\langle \mu^2\rangle/nm^2$ between the CCl_4 and C_6H_6 solutions are due to the excluded volume effect and/or specific solvent effect (see Table 7). Benzene is a better solvent for PPS than carbon tetrachloride.[10] They measured dipole moments of atactic PPS samples of number-average molecular weight = 5−6 × 10^3 and obtained essentially the same $\langle \mu^2\rangle/nm^2$ values as a sample of weight-average molecular weight = 5 × 10^5 gave (Table 7). Since the dipole moment exhibited no molecular weight dependence, the polymeric chain was considered to be free from the excluded volume effect. Although the geometrical parameters of PPS (Table 6) slightly deviate from the above symmetries, the bond dipole moments, m_{S-C} = m_{C^*-S} = 1.21 D and m_{C-C^*} = 0.00 D, satisfy the conditions of symmetry. Because the dielectric constant (ϵ = 2.28) of C_6H_6 is almost equal to that (2.24) of CCl_4, the *specific* solvent effect may suggest atomic-level interactions between solute and solvent to change the conformational energies and/or bond dipole moment(s). As shown in Table 8, the dipole moment of PPS is sensitive to changes in E_α and E_β. The experimental $p_\eta^{CC^*}$ values of BMTP exhibit large solvent dependence; the conformational energies may vary with solvent.

The unperturbed state of polymers, depending on temperature, solvent, and composition, has been referred to as the Θ point. When the conformational energies are subject to solvent effects, it is preferable that the Θ state should be regarded not as a point but as a space of n_e dimensions, where n_e is the number of conformational energies. Each polymer has its own Θ space. If the polymer is free from solvent effects, the Θ space converges to a point. As shown above, PPS has the Θ space with a large volume. The configuration-dependent properties of PPS and PES are sensitive to a change in E_σ; the Θ spaces of the polysulfides are elongated in the direction of the σ axis. The individual experiments on PPS, using a variety of solvents, lead us to different positions in its Θ space. This is probably the reason any sets of conformational energies do not satisfy all of the experimental data fully.

Concluding Remarks

The conformational characteristics of unperturbed PPS have been shown to be, in principle, analogous to those of PES; the S−C and C−C bonds prefer the gauche and trans conformations, respectively. In the crystal, isotactic PPS and PPO, being isomorphous, adopt the all-trans form,[8,39] although the conformation is not the most stable form in the Θ state. The unit cell includes "up" and "down" molecular chains. Thus, the dipole moments are canceled out within a chain and between the two chains; the antiparallel dipole−dipole interactions may somewhat stabilize the crystal structure. However, densities of the PPS and PES crystals are 1.24 and 1.41 g cm^{-3}, respectively.[4,8] The methyl side chain prevents PPS from being packed as closely as PES. As shown before,[2] PEO has only a little energy difference between the tgt and ttt forms in the O−C−C−O bonds. For PPS, PPO, and PEO, therefore, disorderings of the chain structure may begin at comparatively low temperatures, leading to fusion at 53, 73, and 68 °C, respectively. On the other hand, PMS, PMO, and PES are allowed to adopt the most stable conformation in the crystal. The energy minima are ca. −1.05 × 3 (PMS), −1.4 × 3 (PMO), and −1.66 (PES) kcal mol^{-1} per three bonds in depth from the level of the all-trans state. For PMS and PES, the induced dipole−dipole interactions are expected to further stabilize the crystal structure.[1,2] The melting points are as high as 245 °C (PMS), 180 °C (PMO), and 216 °C (PES).

Acknowledgment. This work was supported in part by a Grant-in-Aid for Scientific Research (C) (14550842) of the Japan Society for the Promotion of Science.

Appendix: Statistical Weight Matrices for *R* → *R*, *R* → *S*, *S* → *S*, and *S* → *R* Linkages

The characteristic ratio and dipole moment ratio of atactic PPS were calculated with the following $\mathbf{U}_i$ matrices. When, for example, the $R \rightarrow S$ linkage is formed, $\mathbf{U}_a^{RS}$, $\mathbf{U}_b^{RS}$, and $\mathbf{U}_c^{RS}$ are applied to the (*S*)-repeating unit.

1. *R* → *R* Linkage

$$\mathbf{U}_a^{RR} = \begin{bmatrix} 1 & \sigma & \sigma\zeta & 0 & 0 & 0 & 0 & 0 & 0 \\ 0 & 0 & 0 & 1 & \sigma\zeta & \sigma\zeta & 0 & 0 & 0 \\ 0 & 0 & 0 & 0 & 0 & 0 & 1 & \sigma\zeta & \sigma \\ 1 & \sigma & \sigma\zeta & 0 & 0 & 0 & 0 & 0 & 0 \\ 0 & 0 & 0 & 1 & \sigma\zeta & \sigma\zeta & 0 & 0 & 0 \\ 0 & 0 & 0 & 0 & 0 & 0 & 1 & 0 & \sigma \\ 1 & \sigma & \sigma\zeta & 0 & 0 & 0 & 0 & 0 & 0 \\ 0 & 0 & 0 & 1 & \sigma\zeta & 0 & 0 & 0 & 0 \\ 0 & 0 & 0 & 0 & 0 & 0 & 1 & \sigma\zeta & \sigma \end{bmatrix} \tag{A1}$$

$$\mathbf{U}_b^{RR} = \begin{bmatrix} 1 & \alpha & \beta & 0 & 0 & 0 & 0 & 0 & 0 \\ 0 & 0 & 0 & \tau & \alpha & \beta\omega_2 & 0 & 0 & 0 \\ 0 & 0 & 0 & 0 & 0 & 0 & 1 & 0 & 0 \\ 1 & \alpha & \beta & 0 & 0 & 0 & 0 & 0 & 0 \\ 0 & 0 & 0 & 0 & \alpha & 0 & 0 & 0 & 0 \\ 0 & 0 & 0 & 0 & 0 & 0 & 1 & 0 & 0 \\ 1 & \alpha & \beta & 0 & 0 & 0 & 0 & 0 & 0 \\ 0 & 0 & 0 & 0 & \alpha & 0 & 0 & 0 & 0 \\ 0 & 0 & 0 & 0 & 0 & 0 & 1 & \alpha\omega_1 & \tau\beta \end{bmatrix} \tag{A2}$$

$$\mathbf{U}_c^{RR} = \mathbf{U}_4 \tag{A3}$$

2. *R* → *S* Linkage

$$\mathbf{U}_a^{RS} = \begin{bmatrix} 1 & \sigma & \sigma\zeta & 0 & 0 & 0 & 0 & 0 & 0 \\ 0 & 0 & 0 & 1 & \sigma\zeta & \sigma\zeta & 0 & 0 & 0 \\ 0 & 0 & 0 & 0 & 0 & 0 & 1 & \sigma\zeta & \sigma \\ 1 & \sigma & \sigma\zeta & 0 & 0 & 0 & 0 & 0 & 0 \\ 0 & 0 & 0 & 1 & \sigma\zeta & \sigma\zeta & 0 & 0 & 0 \\ 0 & 0 & 0 & 0 & 0 & 0 & 1 & 0 & \sigma \\ 1 & \sigma & \sigma\zeta & 0 & 0 & 0 & 0 & 0 & 0 \\ 0 & 0 & 0 & 1 & \sigma\zeta & 0 & 0 & 0 & 0 \\ 0 & 0 & 0 & 0 & 0 & 0 & 1 & \sigma\zeta & \sigma \end{bmatrix} \tag{A4}$$

$$\mathbf{U}_b^{RS} = \begin{bmatrix} 1 & \beta & \alpha & 0 & 0 & 0 & 0 & 0 & 0 \\ 0 & 0 & 0 & 1 & \tau\beta & \alpha\omega_1 & 0 & 0 & 0 \\ 0 & 0 & 0 & 0 & 0 & 0 & 0 & 0 & \alpha \\ 1 & \beta & \alpha & 0 & 0 & 0 & 0 & 0 & 0 \\ 0 & 0 & 0 & 1 & 0 & 0 & 0 & 0 & 0 \\ 0 & 0 & 0 & 0 & 0 & 0 & 0 & 0 & \alpha \\ 1 & \beta & \alpha & 0 & 0 & 0 & 0 & 0 & 0 \\ 0 & 0 & 0 & 1 & 0 & 0 & 0 & 0 & 0 \\ 0 & 0 & 0 & 0 & 0 & 0 & \tau & \beta\omega_2 & \alpha \end{bmatrix} \tag{A5}$$

$$\mathbf{U}_c^{RS} = \begin{bmatrix} 1 & \delta & \gamma & 0 & 0 & 0 & 0 & 0 & 0 \\ 0 & 0 & 0 & 1 & \delta & \gamma\omega_2 & 0 & 0 & 0 \\ 0 & 0 & 0 & 0 & 0 & 0 & 1 & \delta\omega_1 & \gamma \\ 1 & \delta & \gamma & 0 & 0 & 0 & 0 & 0 & 0 \\ 0 & 0 & 0 & 1 & \delta & \gamma\omega_2 & 0 & 0 & 0 \\ 0 & 0 & 0 & 0 & 0 & 0 & 1 & 0 & \gamma \\ 1 & \delta & \gamma & 0 & 0 & 0 & 0 & 0 & 0 \\ 0 & 0 & 0 & 1 & 0 & 0 & 0 & 0 & 0 \\ 0 & 0 & 0 & 0 & 0 & 0 & 1 & \delta\omega_1 & \gamma\chi \end{bmatrix} \tag{A6}$$

3. *S* → *S* Linkage

$$\mathbf{U}_{\mathrm{a}}^{SS} = \begin{bmatrix} 1 & \sigma\zeta & \sigma & 0 & 0 & 0 & 0 & 0 & 0 \\ 0 & 0 & 0 & 1 & \sigma & \sigma\zeta & 0 & 0 & 0 \\ 0 & 0 & 0 & 0 & 0 & 0 & 1 & \sigma\zeta & \sigma\zeta \\ 1 & \sigma\zeta & \sigma & 0 & 0 & 0 & 0 & 0 & 0 \\ 0 & 0 & 0 & 1 & \sigma & \sigma\zeta & 0 & 0 & 0 \\ 0 & 0 & 0 & 0 & 0 & 0 & 1 & 0 & \sigma\zeta \\ 1 & \sigma\zeta & \sigma & 0 & 0 & 0 & 0 & 0 & 0 \\ 0 & 0 & 0 & 1 & \sigma & 0 & 0 & 0 & 0 \\ 0 & 0 & 0 & 0 & 0 & 0 & 1 & \sigma\zeta & \sigma\zeta \end{bmatrix} \qquad \text{(A7)}$$

$$\mathbf{U}_{\mathrm{b}}^{SS} = \begin{bmatrix} 1 & \beta & \alpha & 0 & 0 & 0 & 0 & 0 & 0 \\ 0 & 0 & 0 & 1 & 0 & 0 & 0 & 0 & 0 \\ 0 & 0 & 0 & 0 & 0 & 0 & \tau & \beta\omega_2 & \alpha \\ 1 & \beta & \alpha & 0 & 0 & 0 & 0 & 0 & 0 \\ 0 & 0 & 0 & 1 & \tau\beta & \alpha\omega_1 & 0 & 0 & 0 \\ 0 & 0 & 0 & 0 & 0 & 0 & 0 & 0 & \alpha \\ 1 & \beta & \alpha & 0 & 0 & 0 & 0 & 0 & 0 \\ 0 & 0 & 0 & 1 & 0 & 0 & 0 & 0 & 0 \\ 0 & 0 & 0 & 0 & 0 & 0 & 0 & 0 & \alpha \end{bmatrix} \qquad \text{(A8)}$$

$$\mathbf{U}_{\mathrm{c}}^{SS} = \begin{bmatrix} 1 & \delta & \gamma & 0 & 0 & 0 & 0 & 0 & 0 \\ 0 & 0 & 0 & 1 & \delta & \gamma\omega_2 & 0 & 0 & 0 \\ 0 & 0 & 0 & 0 & 0 & 0 & 1 & \delta\omega_1 & \gamma \\ 1 & \delta & \gamma & 0 & 0 & 0 & 0 & 0 & 0 \\ 0 & 0 & 0 & 1 & \delta & \gamma\omega_2 & 0 & 0 & 0 \\ 0 & 0 & 0 & 0 & 0 & 0 & 1 & 0 & \gamma \\ 1 & \delta & \gamma & 0 & 0 & 0 & 0 & 0 & 0 \\ 0 & 0 & 0 & 1 & \delta & 0 & 0 & 0 & 0 \\ 0 & 0 & 0 & 0 & 0 & 0 & 1 & \delta\omega_1 & \gamma\chi \end{bmatrix} \qquad \text{(A9)}$$

4. *S* → *R* Linkage

$$\mathbf{U}_{\mathrm{a}}^{SR} = \begin{bmatrix} 1 & \sigma\zeta & \sigma & 0 & 0 & 0 & 0 & 0 & 0 \\ 0 & 0 & 0 & 1 & \sigma & \sigma\zeta & 0 & 0 & 0 \\ 0 & 0 & 0 & 0 & 0 & 0 & 1 & \sigma\zeta & \sigma\zeta \\ 1 & \sigma\zeta & \sigma & 0 & 0 & 0 & 0 & 0 & 0 \\ 0 & 0 & 0 & 1 & \sigma & \sigma\zeta & 0 & 0 & 0 \\ 0 & 0 & 0 & 0 & 0 & 0 & 1 & 0 & \sigma\zeta \\ 1 & \sigma\zeta & \sigma & 0 & 0 & 0 & 0 & 0 & 0 \\ 0 & 0 & 0 & 1 & \sigma & 0 & 0 & 0 & 0 \\ 0 & 0 & 0 & 0 & 0 & 0 & 1 & \sigma\zeta & \sigma\zeta \end{bmatrix} \qquad \text{(A10)}$$

$$\mathbf{U}_{\mathrm{b}}^{SR} = \begin{bmatrix} 1 & \alpha & \beta & 0 & 0 & 0 & 0 & 0 & 0 \\ 0 & 0 & 0 & 0 & \alpha & 0 & 0 & 0 & 0 \\ 0 & 0 & 0 & 0 & 0 & 0 & 1 & \alpha\omega_1 & \tau\beta \\ 1 & \alpha & \beta & 0 & 0 & 0 & 0 & 0 & 0 \\ 0 & 0 & 0 & \tau & \alpha & \beta\omega_2 & 0 & 0 & 0 \\ 0 & 0 & 0 & 0 & 0 & 0 & 1 & 0 & 0 \\ 1 & \alpha & \beta & 0 & 0 & 0 & 0 & 0 & 0 \\ 0 & 0 & 0 & 0 & \alpha & 0 & 0 & 0 & 0 \\ 0 & 0 & 0 & 0 & 0 & 0 & 1 & 0 & 0 \end{bmatrix} \qquad \text{(A11)}$$

$$\mathbf{U}_{\mathrm{c}}^{SR} = \begin{bmatrix} 1 & \gamma & \delta & 0 & 0 & 0 & 0 & 0 & 0 \\ 0 & 0 & 0 & 1 & \gamma & \delta\omega_1 & 0 & 0 & 0 \\ 0 & 0 & 0 & 0 & 0 & 0 & 1 & \gamma\omega_2 & \delta \\ 1 & \gamma & \delta & 0 & 0 & 0 & 0 & 0 & 0 \\ 0 & 0 & 0 & 1 & \gamma\chi & \delta\omega_1 & 0 & 0 & 0 \\ 0 & 0 & 0 & 0 & 0 & 0 & 1 & 0 & 0 \\ 1 & \gamma & \delta & 0 & 0 & 0 & 0 & 0 & 0 \\ 0 & 0 & 0 & 1 & \gamma & 0 & 0 & 0 & 0 \\ 0 & 0 & 0 & 0 & 0 & 0 & 1 & \gamma\omega_2 & \delta \end{bmatrix} \qquad \text{(A12)}$$

Symbols and Abbreviations

α_r = expansion factor for end-to-end distance
α_u = expansion factor for dipole moment
B3LYP = Becke's three-parameter hybrid functional using the Lee–Yang–Parr correlation functional
BMTP = 1,2-bis(methylthio)propane
ΔG_k = Gibbs free energy
ΔH_{vap} = enthalpy of vaporization
ΔS_{vap} = entropy of vaporization
DMEDT = 2-(1,1-dimethylethyl)-1,4-dithiane
DMP = 1,2-dimethoxypropane
DMSO = dimethyl sulfoxide
E_ξ = conformational energy
η = conformation (t, g^+, or g^-)
HF = Hartree–Fock method
i = bond number
^3J = vicinal coupling constant
$^3J_{AC}$ = ^3J between protons A and C
$^3J_{BC}$ = ^3J between protons B and C
$^3J_{CHA}$ = ^3J between carbon 1 and proton A
$^3J_{CHB}$ = ^3J between carbon 1 and proton B
$^3J_{CHC}$ = ^3J between carbon 6 and proton C
$^3J_G^{CH}$ = ^3J between carbon and proton in gauche position
$^3J_G^{HH}$ = ^3J between protons in gauche position
$^3J_T^{CH}$ = ^3J between carbon and proton in trans position
$^3J_T^{HH}$ = ^3J between protons in trans position
k = conformer
l = bond length
$\vec{\mu}$ = dipole moment vector
$\langle\mu^2\rangle/nm^2$ = dipole moment ratio
μ_k^{BOND} = dipole moment calculated from bond dipole moments
μ_k^{MO} = dipole moment evaluated from MO calculations
m = bond dipole moment
m_{C-C^*} = C–C* bond dipole moment
m_{C^*-S} = C*–S bond dipole moment
MO = molecular orbital
MP2 = second-order Møller–Plesset perturbation theory
m_{S-C} = S–C bond dipole moment
ν = chemical shift
n = number of skeletal bonds
n_e = number of conformational energies
n_S = lone pair of sulfur
ϕ = dihedral angle
PEO = poly(ethylene oxide)
PES = poly(ethylene sulfide)
p_η^{SC} = bond conformation in S–C bond
$p_\eta^{CC^*}$ = bond conformation in C–C* bond
$p_\eta^{C^*S}$ = bond conformation in C*–S bond
PMO = poly(methylene oxide)
PMS = poly(methylene sulfide)
PPO = poly(propylene oxide)
PPS = poly(propylene sulfide)
P_R = (R)-monomer fraction in an atactic PPS chain
r = end-to-end distance of polymer
R = gas constant
$\vec{r}$ = end-to-end vector

$\langle r^2\rangle_0/nl^2$ = characteristic ratio in the Θ state
RIS = rotational isomeric state
σ^*_{C-C} = antibonding orbital of C−C bond
σ^*_{C-S} = antibonding orbital of C−S bond
SCF = self-consistent field
S_{conf} = configurational entropy
T = absolute temperature
T_{bp} = boiling point
$\mathbf{U}_i$ = statistical weight matrix
ξ = intramolecular interaction and statistical weight, i.e., α, β, γ, δ, σ, ω_1, ω_2, τ, ζ, or χ
x = degree of polymerization

References and Notes

(1) Sawanobori, M.; Sasanuma, Y.; Kaito, A. *Macromolecules* **2001,** *34,* 8321.
(2) Sasanuma, Y.; Ohta, H.; Touma, I.; Matoba, H.; Hayashi, Y.; Kaito, A. *Macromolecules* **2002,** *35,* 3748.
(3) Reed, A. E.; Curtiss, L. A.; Weinhold, F. *Chem. Rev.* **1988,** *88,* 899.
(4) Takahashi, Y.; Tadokoro, H.; Chatani, Y. *J. Macromol. Sci., Phys.* **1968,** *B2,* 361.
(5) Tadokoro, H.; Chatani, Y.; Yoshihara, T.; Tahara, S.; Murahashi, S. *Makromol. Chem.* **1964,** *73,* 109.
(6) Takahashi, Y.; Sumita, I.; Tadokoro, H. *J. Polym. Sci., Polym. Phys. Ed.* **1973,** *11,* 2113.
(7) Abe, A. *Macromolecules* **1980,** *13,* 546.
(8) Sakakihara, H.; Takahashi, Y.; Tadokoro, H.; Sigwalt, P.; Spassky, N. *Macromolecules* **1969,** *2,* 515.
(9) For details of properties of PPS, see, e.g., Masamoto, J. Poly(propylene sulfide). In *Polymer Data Handbook;* Mark, J. E., Ed.; Oxford University Press: New York, 1999; p 792.
(10) Nash, D. W.; Pepper, D. C. *Polymer* **1975,** *16,* 105.
(11) Riande, E.; Boileau, S.; Hemery, P.; Mark, J. E. *Macromolecules* **1979,** *12,* 702.
(12) Riande, E.; Boileau, S.; Hemery, P.; Mark, J. E. *J. Chem. Phys.* **1979,** *71,* 4206.
(13) Starks, C. M.; Liotta, C. *Phase Transfer Catalysis: Principles and Techniques;* Academic Press: New York, 1978; Chapter 4.
(14) Frisch, M. J.; Trucks, G. W.; Schlegel, H. B.; Scuseria, G. E.; Robb, M. A.; Cheeseman, J. R.; Zakrzewski, V. G.; Montgomery, J. A., Jr.; Stratmann, R. E.; Burant, J. C.; Dapprich, S.; Millam, J. M.; Daniels, A. D.; Kudin, K. N.; Strain, M. C.; Farkas, O.; Tomasi, J.; Barone, V.; Cossi, M.; Cammi, R.; Mennucci, B.; Pomelli, C.; Adamo, C.; Clifford, S.; Ochterski, J.; Petersson, G. A.; Ayala, P. Y.; Cui, Q.; Morokuma, K.; Malick, D. K.; Rabuck, A. D.; Raghavachari, K.; Foresman, J. B.; Cioslowski, J.; Ortiz, J. V.; Baboul, A.; Stefanov, B. B.; Liu, G.; Liashenko, A.; Piskorz, P.; Komaromi, I.; Gomperts, R.; Martin, R. L.; Fox, D. J.; Keith, T.; Al-Laham, M. A.; Peng, C. Y.; Nanayakkara, A.; Gonzalez, C.; Challacombe, M.; Gill, P. M. W.; Johnson, B. G.; Chen, W.; Wong, M. W.; Andres, J. L.; Gonzalez, C.; Head-Gordon, M.; Replogle, E. S.; Pople, J. A. *Gaussian 98*, revision A.7; Gaussian, Inc.: Pittsburgh, PA, 1998.
(15) Foresman, J. B.; Frisch, Æ. *Exploring Chemistry, with Electronic Structure Methods,* 2nd ed.; Gaussian, Inc.: Pittsburgh, PA, 1996.
(16) Besler, B. H.; Merz, K. M., Jr.; Kollman, P. A. *J. Comput. Chem.* **1990**, *11,* 431.
(17) Singh, U. C.; Kollman, P. A. *J. Comput. Chem.* **1984,** *5,* 129.
(18) Ivin, K. J.; Navrátil, M. *J. Polym. Sci., Part B* **1970,** *8,* 51.
(19) Ivin, K. J.; Navrátil, M. *J. Polym. Sci., Part A-1* **1971,** *9,* 1.
(20) Flory, P. J. *Statistical Mechanics of Chain Molecules;* Wiley Interscience: New York, 1969.
(21) Mattice, W. L.; Suter, U. W. *Conformational Theory of Large Molecules: The Rotational Isomeric State Model in Macromolecular Systems;* Wiley & Sons: New York, 1994.
(22) Xu, J.; Song, X.; Zhou, Z.; Yan, D. *J. Polym. Sci., Polym. Phys. Ed.* **1991,** *29,* 877.
(23) Sasanuma, Y. *Macromolecules* **1995,** *28,* 8629.
(24) Law, R. V.; Sasanuma, Y. *Macromolecules* **1998,** *31,* 2335.
(25) Riande, E.; Saiz, E. *Dipole Moments and Birefringence of Polymers*; Prentice Hall: Englewood Cliffs, NJ, 1992.
(26) Abe, A. *Macromolecules* **1980,** *13,* 541.
(27) Nelder, J. A.; Mead, R. *Comput. J.* **1965,** *7,* 308.
(28) Becker, R. H. M. S. Thesis in Chemistry, The Polytechnic Institute of Brooklyn, Brooklyn, NY, 1967.
(29) Mark, J. E. *Rubber Chem. Technol.* **1973,** *46,* 593.
(30) Rahalkar, R. R.; Mark, J. E.; Boileau, S.; Hemery, P.; Riande, E. *J Polym. Sci., Polym. Phys. Ed.* **1979,** *17,* 1623.
(31) Sepulchre, M.; Spassky, N.; Van Ooteghem, D.; Goethals, E, J. *J. Polym. Sci., Polym. Chem. Ed.* **1974,** *12,* 1683.
(32) Abe, A.; Hirano, T.; Tsuruta, T. *Macromolecules* **1979,** *12,* 1092.
(33) Brant, D. A.; Miller, W. G.; Flory, P. J. *J. Mol. Biol.* **1967,** *23,* 47.
(34) Tonelli, A. E. *J. Chem. Phys.* **1970,** *52,* 4749.
(35) Tonelli, A. E. *J. Chem. Phys.* **1970,** *53,* 4339.
(36) Mark, J. E. *J. Chem. Phys.* **1977,** *67,* 3300.
(37) Nagai, K.; Ishikawa, T. *Polym. J.* **1971,** *2,* 416.
(38) Doi, M. *Polym. J.* **1970,** *3,* 252.
(39) Cesari, M.; Perego, G.; Marconi, W. *Makromol. Chem.* **1966,** *94,* 194.

MA020730M